JOURNAL OF AIRCRAFT
Vol. 29, No. 6, Nov.–Dec. 1992

Effects of Fuselage Boundary Layer on Noise Propagation from Advanced Propellers

Peter L. Spence*
Lockheed Engineering and Sciences Company, Hampton, Virginia 23666

A computer program has been developed that models refractive and scattering effects on acoustic pressure waves propagating through a boundary layer, encompassing an aircraft's fuselage. The periodic noise source is generated by a propeller and is assumed to be known. The fuselage is represented by an infinitely long cylinder embedded in a longitudinal flow. For a specified boundary-layer velocity profile and thickness, the program calculates the acoustic pressure at the surface of the cylinder, given the incident field at the top of the boundary layer. Numerical experiments illustrate the importance of describing the boundary-layer velocity profile shape and thickness as accurately as possible. Computational results are compared with flight test data measured during the Propfan test assessment (PTA) experiment. Comparisons of theoretical results with the measured data show good agreement.

Nomenclature

a_o = cylinder radius, m
c = speed of sound, re c_o
c_c = speed of sound at cylinder's surface, re c_o
c_o = freestream speed of sound, m/s
c_∞ = freestream speed of sound, re $c_o(c_\infty = 1)$
$H_\nu^{(1)}$ = Hankel function of the first kind of order ν
J_ν = Bessel function of the first kind of order ν
k_r = radial wave number
k_x = axial wave number
M_∞ = freestream Mach number
m = harmonic index in circumferential direction
N_b = number of propeller blades
N_x = number of axial grid points
N_θ = number of circumferential grid points
n = harmonic blade-passing frequency
P = acoustic pressure, re $\rho_o c_o^2$
R_c = cylinder radius, re $a_o(R_c = 1)$
R_s = distance from propeller axis to point of closest blade approach at the top of the boundary layer around cylinder, re a_o
R_δ = distance from center of cylinder to top of boundary layer, re a_o
$R_{\delta s}$ = distance between propeller and cylinder center, $(R_\delta + R_s)$
r = radial coordinate, re a_o
r_p = propeller-centered radial coordinate, re a_o
T = blade-passing period
t = time, re a_o/c_o
U = axial velocity, re c_o
U_∞ = freestream axial velocity, re c_o
x = axial coordinate, re a_o
δ = boundary-layer thickness, re a_o
ζ = boundary-layer coordinate, re δ
θ = angular coordinate, on cylinder
Π = acoustic pressure in Fourier transformed space
ρ_o = freestream density, kg/m^3
ψ = angular coordinate on propeller
Ω = rotational velocity of propeller
ω = radian frequency
$(\,)'$ = radial derivative

Introduction

IN many problems of helicopter rotor and propeller acoustics, the noise is measured under a boundary layer. It has been shown that the propagation effects through the boundary layer are significant and should be included in noise predictions. McAninch and Rawls[1] presented results for a flat-plate model that showed a significant reduction of the "free-field-plus-6 dB" noise prediction forward of the plane of the propeller. In the realistic case of a curved fuselage, the study of wave propagation in the boundary layer becomes complex, particularly when numerical calculations are involved. Hanson and Magliozzi[2] modeled an infinitely long cylinder with an isothermal thin boundary layer and found the same shielding effects forward of the propeller. Further analysis by Lu[3] dropped the restrictions requiring the boundary layer to be isothermal and thin with respect to the fuselage diameter. In this work, however, a laminar boundary-layer velocity profile was used.[1-3] This article describes the results of a computer program based on the analytic results of McAninch[1] for an infinitely long cylinder that includes a turbulent boundary-layer velocity profile option.

In order to compute the propagation effects on the noise due to the velocity gradient in the boundary layer, the shear-flow-wave equation must be solved. This is a linear homogeneous ordinary differential equation with variable coefficients. Singularities can occur in the computational domain. Near the region of the singular points, the computational domain is analytically continued into the complex plane.[1] The shear-flow-wave equation is solved by integrating from the fuselage surface (assuming unit pressure and zero admittance initially) to the top of the boundary layer using standard fourth-order Runge-Kutta integration techniques. The resulting acoustic pressure and velocity are then used along with the free-field incident pressure to compute the actual surface acoustic pressure. This is accomplished by using a transfer function derived from Bessel's equation that governs the acoustic propagaton outside the boundary layer.

Computational results are compared with data measured on the Propfan test assessment (PTA) aircraft.[4,5] PTA acoustic data were measured by microphones placed flush along the side of the fuselage and along an acoustic boom cantilevered on the port wing. Although the data measured on the acoustic boom are assumed to be free of boundary-layer effects, the computer program is applied to predict the effect of scattering of the incident waves. Data measured on the

Received April 13, 1991; revision received Oct. 29, 1991; accepted for publicaton Oct. 29, 1991.

*Senior Engineer, Acoustics and Dynamics Department, 144 Research Drive. Member AIAA.

fuselage are influenced by the presence of a boundary-layer, and calculations made there include both refraction and scattering.

Theoretical Formulation

The problem to be solved is illustrated in Fig. 1. An aircraft fuselage is modeled by an infinitely long cylinder of radius a_o immersed in an axially directed uniform flow, U. A propeller whose axis of rotation is parallel to the centerline of the cylinder acts as the exterior noise source and is axisymmetric and periodic. The coordinate system has its origin at the center of the cylinder in the plane containing the propeller. Around the cylinder is a boundary layer of thickness δ whose velocity gradient refracts the incident acoustic waves from the noise source. Due to the presence of this velocity gradient, from $U = 0$ at the cylinder's surface to the uniform freestream velocity (U_∞) at the boundary-layer edge, some waves are refracted out of the boundary layer before reaching the surface of the cylinder. Acoustic waves striking the surface of the cylinder are scattered according to an admittance criteria which can be specified as a function of the propagating frequency of the incident noise source. Also, it is assumed that the sound speed and axial velocity profile are only dependent upon the radial coordinate r, thus, $U = U(r)$ and $c = c(r)$. The goal is to calculate the surface acoustic pressure on the cylinder given the incident acoustic pressure at the edge of the cylinder's boundary layer. In order to do so, the equations governing the conservation of mass, energy, and momentum within the boundary layer must be solved.

In the shear layer surrounding the cylinder, the governing equation in cylindrical coordinates derived in Goldstein[6] is

$$\frac{D}{Dt}\left[\nabla^2 P + \frac{2c'}{c}\frac{\partial P}{\partial r} - \frac{1}{c^2}\frac{D^2 P}{Dt^2}\right] - 2U'\frac{\partial^2 P}{\partial r \partial x} = 0 \quad (1)$$

where

$$\nabla^2 = \frac{1}{r}\frac{\partial}{\partial r} + \frac{\partial^2}{\partial r^2} + \frac{1}{r^2}\frac{\partial^2}{\partial \theta^2} + \frac{\partial^2}{\partial x^2}$$

and the convective derivative is

$$\frac{D}{Dt} = \frac{\partial}{\partial t} + U\frac{\partial}{\partial x}$$

Substituting solutions of the form

$$P(r, x, \theta, t) = \Pi(r)e^{ik_x x + im\theta - i\omega t}$$

yields the form of the shear-flow-wave equation to be solved numerically

$$(\omega - Uk_x)\Pi'' + \left[(\omega - Uk_x)\left(\frac{1}{r} + \frac{2c'}{c}\right) + 2U'k_x\right]\Pi' + (\omega - Uk_x)\left[\left(\frac{\omega - Uk_x}{c}\right)^2 - k_x^2 - \left(\frac{m}{r}\right)^2\right]\Pi = 0 \quad (2)$$

The velocity gradient within the shear layer $U(r)$ defines the boundary-layer velocity profile. In this study, a laminar and a turbulent velocity profile were used. Pohlhausen's[7] profile is used for the laminar case

$$U = U_\infty[\zeta^4 - 2\zeta^3 + 2\zeta] \quad (3)$$

and the one-seventh power law is used for the turbulent case

$$U = U_\infty \zeta^{1/7} \quad (4)$$

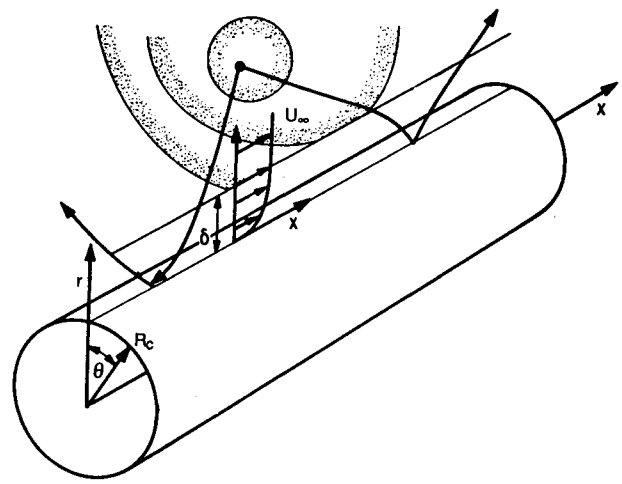

Fig. 1 Circular cylinder model and coordinate system.

Here, the boundary-layer coordinate ζ is used to specify U and c

$$\zeta = [(r - R_c)/\delta] \quad (5)$$

Outside of the boundary layer around the cylinder, where the axial flow speed and the speed of sound become constant, Eq. (2) reduces to

$$\Pi'' + \frac{1}{r}\Pi' + \left[\left(\frac{\omega}{c_\infty} - M_\infty k_x\right)^2 - k_x^2 - \left(\frac{m}{r}\right)^2\right]\Pi = 0 \quad (6)$$

The solutions to Eq. (6) for the propeller-centered coordinate system, are Hankel functions of the first kind, that satisfies the boundary condition that all waves are propagating outward from the source. The incident acoustic pressure on the cylinder generated by the propeller, is computed from the time domain formulation of the Ffowcs Williams-Hawkings equation, Farassat.[8] The computer program ASSPIN[9] (advanced subsonic and supersonic propeller induced noise, formerly DFP-ATP) was used to numerically compute the acoustic pressure signature P for each observer location at the top of the boundary layer of the cylinder. The sound harmonic of this pressure P_n was obtained by Fourier transforming P over the blade-passing period T

$$P_n = \frac{1}{2\pi}\int_0^T P e^{i\omega t}\, dt \quad (7)$$

The radian frequency ω is given by $nN_b\Omega$. For convenience, the amplitude of the outward propagating wave can be determined from Π_s, where Π_s is Π defined at the top of the cylinder's boundary layer—along the axial line—parallel to the propeller's axis of rotation, and at the point of closest blade approach to the cylinder

$$\Pi_s(R_s) = \frac{1}{2\pi}\int_{-\infty}^{\infty} P_n(R_s)e^{-ik_x x}\, dx \quad (8)$$

To specify the incident wave at the top of the boundary layer everywhere around the cylinder, as well as to convert from the propeller-centered coordinate system to the cylinder-centered coordinate system, the Hankel identity (Graf's Theorem,[10] Fig. 2) is implemented

$$H^{(1)}_{nN_b}(k_r r_p)e^{inN_b\psi} = \sum_{m=-\infty}^{\infty} H^{(1)}_{nN_b+m}(k_r R_{\delta s})J_m(k_r R_\delta)e^{im\theta} \quad (9)$$

Here

$$k_r = \sqrt{\left(\frac{\omega}{c_\infty} - M_\infty k_x\right)^2 - k_x^2}$$

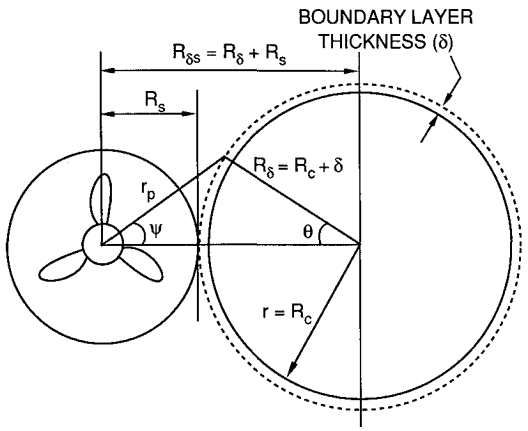

Fig. 2 Relationship between lengths used in Graf's theorem.

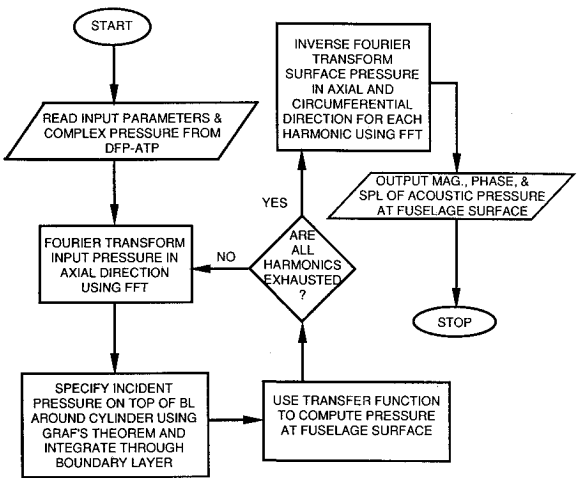

Fig. 3 Flow chart of solution procedure.

Following the procedure outlined in the first three references, the incident and scattered acoustic waves at the top of the boundary layer are matched with the waves computed by numerically integrating Eq. (2) using a fourth-order Runge-Kutta integration scheme. Singular points are encountered during the integration when the coefficient of the highest order derivative of Eq. (2) goes to zero. In this event the computational domain is analytically continued into the complex plane.[1] The initial conditions for the integration at the cylinder's surface are unit pressure and zero admittance. Although the admittance can be specified at input as a function of ω, all results reported here use zero admittance for all values of ω. This represents the case of a hard, perfectly reflecting surface.

Solution Procedure

A general flow chart of the solution procedure is shown in Fig. 3. All Fourier transforms and inverse transforms are done making use of fast Fourier transform (FFT) techniques. ASSPIN is used to compute the incident pressure on the cylinder. This incident pressure is specified along a line of equally spaced grid points, parallel to the propeller hub axis at the point of closest blade approach, along the cylinder on top of the boundary layer. Due to the use of the FFT, the number of grid points must be the result of 2^j, where j is a positive integer. Further, once discretization occurs for programming on a computer, the number and range of the grid points must adequately resolve the phase variation along this axial grid.

Theory Validation

PTA Experiment

As a means of validating the results of the computer program, measured results from the PTA experiment are used to compare with predictions. The PTA experiment was conducted by Lockheed Aeronautical Systems Company and NASA Lewis Research Center between 1984–1988.[4,5] The objective of the experiment was to determine the aerodynamic response and the acoustic impact of an advanced propfan on an aircraft. The aircraft was a modified Gulfstream GII illustrated schematically in Fig. 4. Mounted on the port wing was an eight-bladed, 2.74-m- (9-ft) diam SR7-L propfan that rotated up inboard with respect to the fuselage. Outboard of the propfan was an acoustic boom cantilevered near the tip of the wing.

The PTA aircraft was fitted with over 100 transducers, but what is of interest to this study is the acoustic data measured by microphones mounted flush on the fuselage surface. Specifically for this report, noise predictions will be compared with the nine fuselage microphones located along a line parallel to the propeller's rotational axis at the point of closest blade approach. This line of microphones will be referred to as the fuselage side array. Also, noise predictions will be compared with the 11 microphones around the fuselage in the rotational plane of the propeller. These microphones will be referred to as the circumferential belt array. The propfan lies an equal distance between the point of closest blade approach along the fuselage and the corresponding point on the acoustic boom. The distance from these surfaces to the tip of the propeller is 1.70 m (5.58 ft). Further, the locations of the five boom microphones mirror the locations of five of the microphones on the fuselage side array.

References 4 and 5 contain more detail about the test flights and the aircraft's configuration. Some analysis of the measured data trends can be found in Ref. 11, and Dunn and Farassat[12] provide a description of how the loading on the propeller was calculated for ASSPIN.

The operating conditions corresponding to the PTA design conditions are used to demonstrate the use of the developed program. These conditions are listed in Table 1. With a fundamental blade passing frequency (BPF) of 226 Hz and a freestream speed of sound of 299 m/s (982 ft/s), the corresponding fundamental wave length of the propagating wave is 1.3 m (4.3 ft). Because the boom is conical shaped, its diameter ranges from 18.80 cm (7.40 in.) at its base under

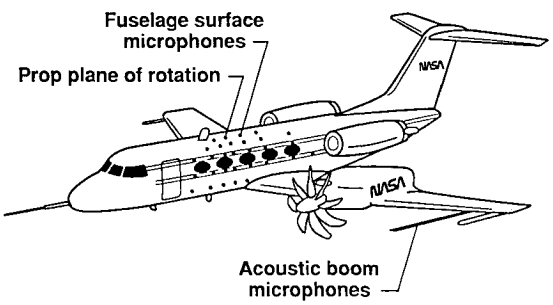

Fig. 4 PTA aircraft.

Table 1 PTA flight conditions used in the study

	Design condition	Lower forward flight speed condition
Flight Mach number, M_∞	0.813	0.605
Rotation tip Mach number	0.814	0.763
Helical tip Mach number	1.150	0.974
BPF, Hz	226.13	213.87
Altitude, km (ft)	10.7 (35,000)	10.7 (35,000)
Speed of sound, c_o, m/s (ft/s)	299.3 (982.0)	301.9 (990.5)
Density, ρ_o, kg/m^3 (slug/ft^3)	0.372 (7.22E-4)	0.369 (7.15E-4)

the port wing to 2.90 cm (1.14 in.) at its tip forward of the wing. The diameter of the fuselage is 2.39 m (7.83 ft). Since the fundamental wavelength is so much larger than the medium diameter of the boom, it is assumed that any boundary layer enveloping the boom would have essentially no refractive effect on the incident acoustic pressure wave field. However, scattering must still be considered. Although the boundary layer on the fuselage was not measured for thickness or profile, the relative wavelengths and diameter of the fuselage indicate that a boundary layer on the fuselage would have an effect on the incident acoustic wave field. From Schlichting's[13] flat-plate approximation, an estimate to the turbulent boundary-layer thickness was found to be on the order of 10 cm (4 in.).

Computational Results

Incident Acoustic Pressure

Before calculating the acoustic pressure at the fuselage surface, the incident pressure at the top of the boundary layer was verified as being properly specified around the cylinder. In Fig. 5 are plotted comparisons between the free-field noise predicted by ASSPIN at $\theta = 0$ deg (the point of closest approach), and $\theta = 180$ deg (the opposite or far-side of the fuselage) with that reconstructed from the prediction at $\theta = 0$ deg using Graf's theorem. The magnitude of the acoustic pressure is given in sound pressure level (SPL) where

$$\text{SPL} = 20 \log_{10}(P \cdot \rho_o c_o^2 / 20\ \mu\text{Pa})$$

These results for the first harmonic of the BPF show excellent agreement. The oscillations at the ends farther than one propeller diameter away from the propeller plane, are due to performing the FFT with a discontinuity at the end points (Gibbs phenomenon) of the predication at $\theta = 0$ deg. The grid used for the results shown in Fig. 5 was 128 axial (N_x) by 32 circumferential (N_θ) points. Numerical experiments were conducted to determine the proper grid resolution required to resolve the incident pressure at the top of the boundary layer for higher harmonics. It was found that although $N_x = 128$ by $N_\theta = 32$ was adequate for the first harmonic, both the second and third required a grid of $N_x = 256$ by $N_\theta = 64$ grid points.

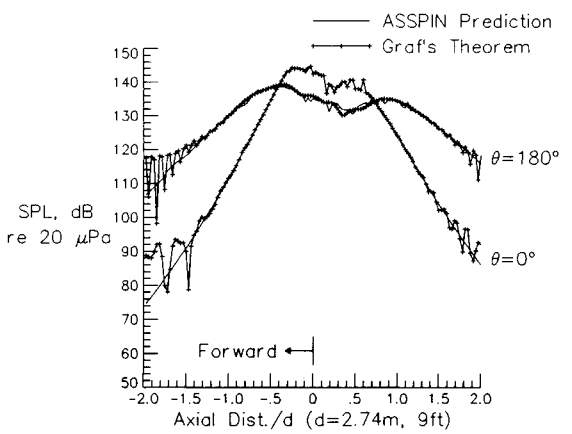

Fig. 5 Reconstruction of the incident acoustic pressure using Graf's theorem.

Fuselage Surface Noise vs Boundary-Layer Profile

To compute the acoustic pressure at the surface of the fuselage, a boundary-layer velocity profile must be specified. Two velocity profiles are shown in the insert of Fig. 6. No velocity gradient is specified when a scattering-only calculation is made. Shown in the insert are the laminar (Eq. (3)) and the turbulent (Eq. (4)) velocity profiles. For the design operating conditions given in Table 1, surface acoustic pressure results for these velocity profiles are shown in Fig. 6 along with the incident pressure at $\theta = 0$ deg. A 10-cm (4-in.) boundary-layer thickness, δ, was used. Although the sound speed profile within the boundary layer also can be specified, all results presented here assume no gradient in the sound speed. Further, to smooth the high-frequency oscillations at the ends of the axial computational domain, a running average filter was applied to the computed surface acoustic pressure.

As can be seen in Fig. 6, the scattering-only case resulted in the nearly constant 6 dB above the incident pressure. This indicates pressure-doubling at the fuselage surface that would be expected since there is no axial velocity gradient to refract the incident waves. The other three profiles also show the nearly constant 6 dB increase over the incident pressure in the aft region only. Forward of the plane of the propeller, the laminar profile shows a great deal of shielding or decrease in noise levels due to incoming pressure waves being refracted in the boundary-layer before reaching the fuselage surface. Even though the turbulent boundary-layer velocity gradient is quite large near the cylinder (fuselage) surface, its velocity gradient is much smaller than the laminar velocity gradient throughout most of the width of the boundary layer. Because of this, less refraction occurs within the boundary layer using the turbulent boundary-layer velocity profile and the shielding of the incident noise is not as prevalent. This relates to boundary-layer theory where a shape factor is defined by a ratio of the boundary-layer displacement thickness to its momentum thickness.[13] The laminar profile has a larger shape factor than the turbulent profile. From these calculations the acoustic shielding of the surface is directly proportional to the boundary-layer shape factor. Aerodynamically it is logical to assume that the turbulent velocity profile is the proper profile to use

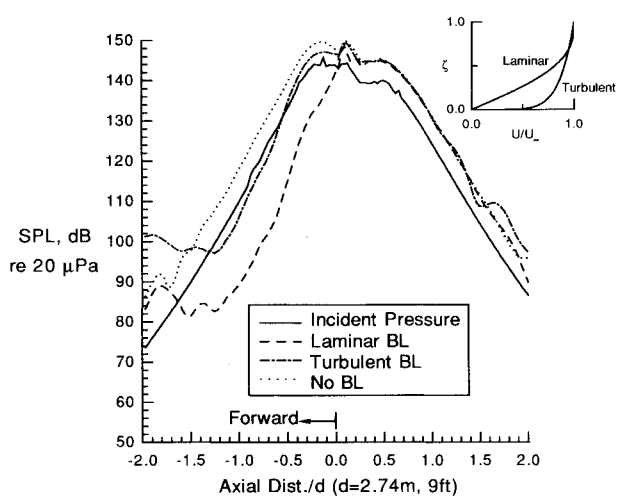

Fig. 6 Scattering and refraction effects vs boundary-layer velocity profile.

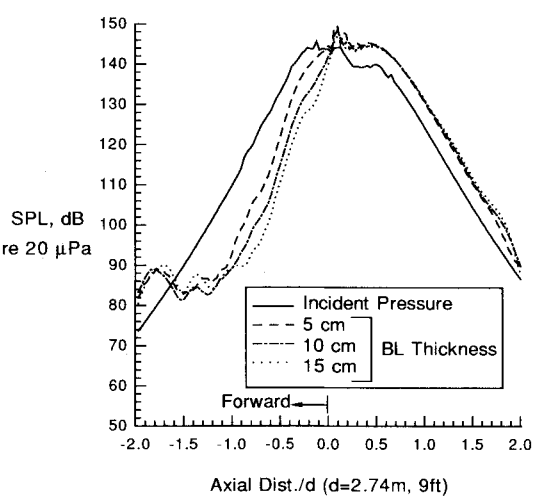

Fig. 7 Scattering and refraction effects vs boundary-layer thickness.

for the high-forward flight Mach numbers (0.813 for this case) used in most of the PTA flight tests.

Fuselage Surface Noise vs Boundary-Layer Thickness

To show the effect of varying boundary-layer thickness, δ, results are plotted in Fig. 7 in the same format as Fig. 6 using the laminar profile for three values of δ. The values taken were 5, 10, and 15 cm (~2, 4, and 6 in.). Figure 7 shows that the thicker the boundary layer, the greater the shielding forward of the propeller plane. Although the boundary-layer thickness has been changed only a few centimeters, the relative change in δ is as great as 200% (5–15 cm). This illustrates the importance of specifying the boundary-layer thickness as accurately as possible since altering the thickness by only a few centimeters has a dramatic effect on the noise forward of the propeller plane.

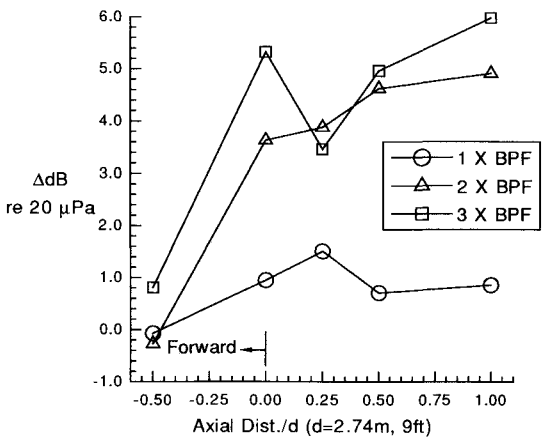

Fig. 8 Acoustic boom scattering vs frequency (BPF = 226 Hz).

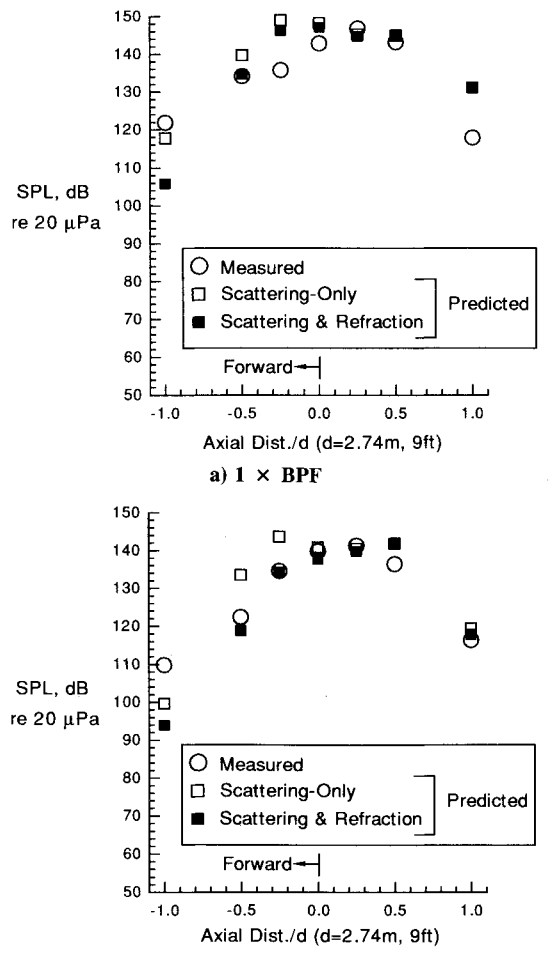

a) 1 × BPF

b) 2 × BPF (BPF = 226 Hz)

Fig. 9 Surface acoustic pressure along fuselage side array.

Acoustic Boom Scattering

An application of a scattering-only calculation was made for the boom microphones for the first three harmonics of the BPF. The higher resolution grid of $N_x = 256$ and $N_\theta = 64$ was used since three harmonics were calculated. To account for the varying diameter of the boom, the scattering was calculated at each microphone installation using the local diameter on the boom. Referring to Fig. 8, the overall results show the effect of scattering is greater for the shorter wave lengths found in the higher harmonics of the propagating wave field. For all three harmonics, the forward microphone shows little or no noise increase over the free-field prediction due to the small boom diameter, 2.90 cm (1.14 in.) at this microphone location. Even for the third harmonic, where the propagating acoustic wave length is approximately 0.44 m, the diameter of the boom at the forward microphone location is too small to scatter the incident wave field. However, the in-plane microphone and the three aft microphones do show an increase in noise at the boom surface due to surface scattering. At these locations, approximately a 1 dB increase over the free-field prediction is found for the first harmonic, whereas the second harmonic shows an increase of between 3–5 dB and the third is approximately a 5–6 dB increase. These scattering calculations are included in the PTA acoustic-boom-noise predictions found in Ref. 12.

Computational Time

All the computer runs were executed on the CRAY computers at NASA Langley Research Center. It was determined

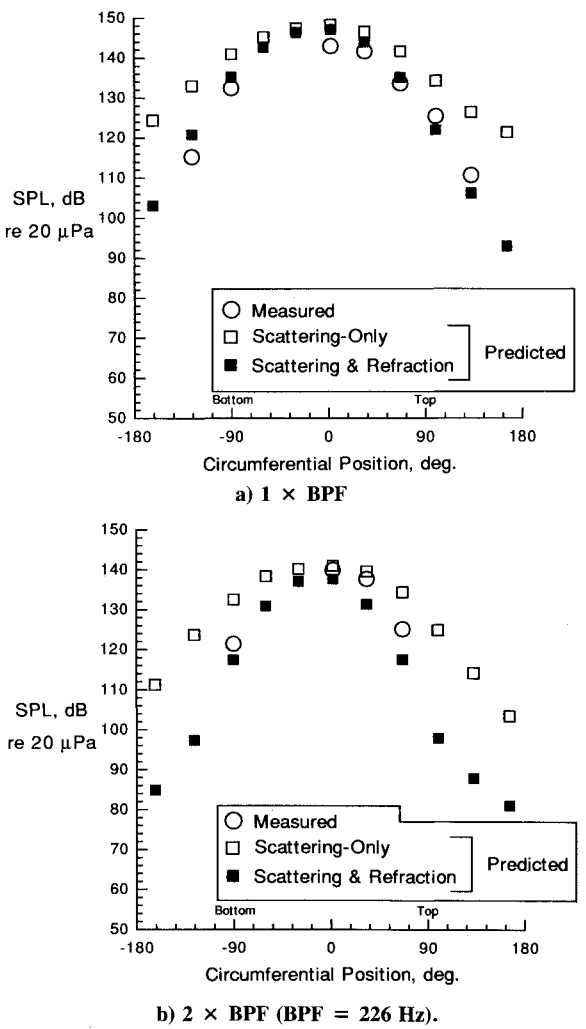

a) 1 × BPF

b) 2 × BPF (BPF = 226 Hz).

Fig. 10 Surface acoustic pressure along circumferential belt array.

that using either a laminar or turbulent boundary-layer velocity profile required approximately 0.016 s/grid point/harmonic to execute the code on the CRAY Y-MP and approximately 0.023 s/grid point/harmonic on the CRAY-2S. When turning off the velocity gradient within the boundary layer and doing a scattering-only calculation, the time required was approximately 0.0058 s/grid point/harmonic on the CRAY Y-MP and 0.0086 s/grid point/harmonic on the CRAY-2S.

Comparison with Measured Results

As stated earlier, noise predictions were compared with measured noise taken from the PTA flight experiment. Comparisons were made for two operating conditions 1) the design condition, 2) and a lower forward flight speed condition (forward Mach number = 0.605). These flight conditions are listed in Table 1. First, measured and predicted values along the fuselage side array are compared. This array of microphones is located along the line parallel to the propeller axis at the point of closest blade approach to the fuselage. The second comparison is between the measured and predicted results along the circumferential belt array lying in the plane of the propeller and encompassing the fuselage. The turbulent boundary-layer profile was used for the predictions with a boundary-layer thickness of 10 cm (4 in.).

Figure 9 shows the first two sound harmonics of the acoustic pressure for the design condition case along the fuselage side array. Two predictions are displayed at each microphone location, both predictions include cylindrical scattering. One of the predicted values also includes refraction due to the presence of a boundary layer whereas the other does not. For both harmonics of the BPF, the inclusion of boundary-layer refraction improves the prediction, especially in the second harmonic. The large measured value of SPL (one propeller diameter forward of the plane of rotation) may be due to nonuniform inflow into the propeller. A steady uniform inflow was assumed for these predictions.

The measured values comparison with prediction for the circumferential belt array is given in Fig. 10. The results of the first harmonic, shown in Fig. 10a, dramatically illustrate the importance of including boundary-layer refraction. There is excellent agreement between the measured and predicted noise levels for both harmonics. It is important to emphasize that both the measured and predicted noise levels are higher below the axial-line-of-closest-approach toward the bottom of the fuselage than those levels found above the axial line toward the top of the fuselage. This asymmetry exits because the propeller rotates up inboard toward the fuselage.

Analogous comparisons were made for the lower forward flight speed listed in Table 1. The measured and predicted comparison along the fuselage side array is shown in Fig. 11. Less refraction occurs forward of the plane of the propeller for this lower forward flight velocity case. This is consistent with McAninch's[14] conclusion for the plane wave case that the acoustic shielding (incident waves refracted out of the boundary-layer before reaching the surface) decreases with frequency and freestream Mach number. The fundamental propagating frequency is fairly constant since it only dropped 5% (226.13–213.87 Hz). However, the freestream Mach number is reduced 25% (0.813–0.605). Again, as with the design condition case, the high measured values found one propeller diameter forward of the plane of the propeller, are believed due to nonuniform inflow into the propeller caused by in-

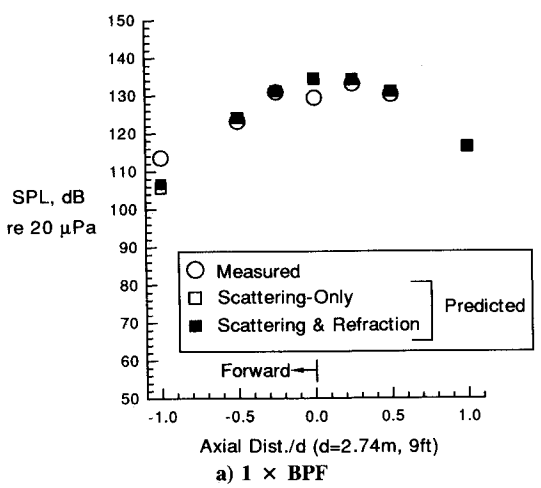

a) 1 × BPF

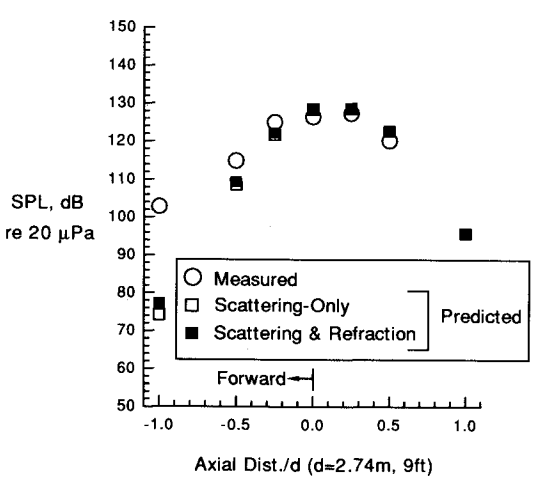

b) 2 × BPF (BPF = 214 Hz).

Fig. 11 Surface acoustic pressure along fuselage side array.

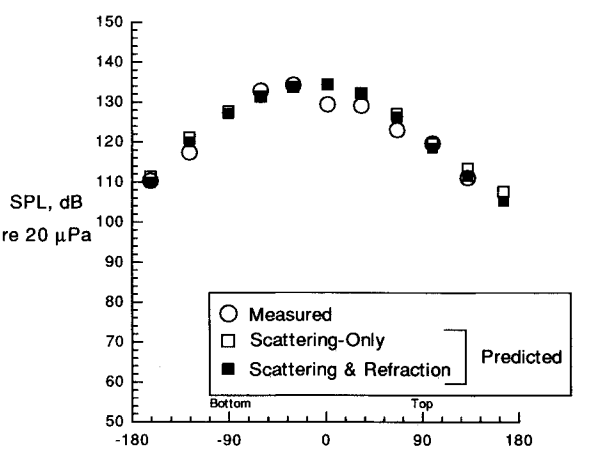

a) 1 × BPF

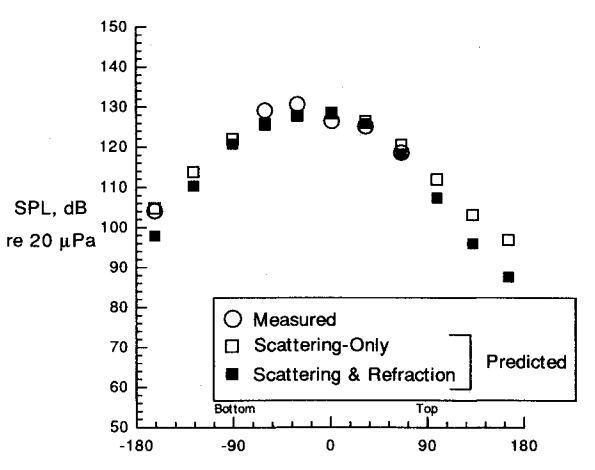

b) 2 × BPF (BPF = 214 Hz).

Fig. 12 Surface acoustic pressure along circumferential belt array.

stallation effects that were not modeled in predicting the incident pressure.

Measured data taken on the circumferential belt array for the lower forward flight speed case is compared with prediction in Fig. 12. As with the higher speed case, the agreement is excellent for the two harmonics. Also, almost no refraction is evidenced in the first sound harmonic except at the far (shadow) side of the fuselage. More refraction occurs in the second harmonic.

Concluding Remarks

A computer program has been written, validated, and its theory documented which can compute the effect on noise propagating through a boundary layer. Scattering of the incident acoustic pressure waves off cylindrical bodies is included in the computer program. The inclusion of boundary-layer refraction and scattering from a cylindrical surface has been shown to have a dramatic effect on the noise levels predicted under a boundary layer. The results presented here demonstrate that it is not sufficient to simply add 6 dB to free-field predictions to represent a prediction on a hard surface, when the surface is embedded in as flow, or when that surface is highly curved.

The resulting boundary-layer refraction is dependent on both the shape and thickness of the specified boundary-layer velocity profile. The thicker the boundary layer, the greater the amount of shielding of the incident waves. Based on the calculations contained within the paper, the acoustic shielding of the surface varies directly with the boundary-layer velocity profile shape factor.

There is good agreement between the predicted noise levels and the PTA measured noise levels, especially in the circumferential directivity. Results show that adding refraction effects to a scattering-only prediction improves the comparison between the measured and predicted noise levels.

References

[1]McAninch, G. L., and Rawls, J. W., "Effects of Boundary Layer Refraction and Fuselage Scattering on Fuselage Surface Noise From Advanced Turboprop Propellers," AIAA Paper 84-0249, Jan. 1984.

[2]Hanson, D. B., and Magliozzi, B., "Propagation of Propeller Tone Noise Through a Fuselage Boundary Layer," *Journal of Aircraft*, Vol. 22, No. 1, 1985, pp. 63–70.

[3]Lu, H., "Fuselage Boundary Layer Effects on Sound Propagation and Scattering," AIAA Paper 89-1098, April 1989.

[4]Little, B. H., Bartel, H. W., Reddy, N. N., Swift, G., Withers, C. C., and Brown, P. C., "Propfan Test Assessment (PTA) Flight Test Report," NASA CR 182278, April 1989.

[5]Little, B. H., Poland, D. T., Bartel, H. W., Withers, C. C., and Brown, P. C., "Propfan Test Assessment (PTA) Final Project Report," NASA CR 185138, July 1989.

[6]Goldstein, M. E., "Aeroacoustics," NASA SP-346, 1974.

[7]White, F., *Viscous Fluid Flow*, McGraw-Hill, New York, 1974, pp. 310–311.

[8]Farassat, F., "Prediction of Advanced Propeller Noise in the Time Domain," *AIAA Journal*, Vol. 24, No. 4, 1986, pp. 578–584.

[9]Dunn, M. H., and Tarkenton, G. M., "Users' Manual for the Langley High Speed Propeller Noise Prediction Program (DFP-ATP)," NASA CR 4208, Jan. 1989.

[10]Abramowitz, M., and Stegun, I. A., *Handbook of Mathematical Functions*, National Bureau of Standards, Washington, DC 1964.

[11]Spence, P. L., and Block, P. J. W., "Analysis of the PTA External Noise Data and Comparison with Predictions," AIAA Paper 90-3935, Oct. 1990.

[12]Dunn, M. H., and Farassat, F., "State-of-The-Art of High Speed Propeller Noise Prediction—A Multidisciplinary Approach and Comparison with Measured Noise Data," AIAA Paper 90-3934, Oct. 1990.

[13]Schlichting, H., *Boundary Layer Theory*, 7th ed., McGraw-Hill, New York, 1979, pp. 673–677.

[14]McAninch, G. L., "A Note on Propagation through a Realistic Boundary Layer," *Journal of Sound and Vibration*, Vol. 88, No. 2, 1983, pp. 271–274.